

# 1 Supplementary material

The following supplementary material is included

- Fig. 1, showing confidence regions for  $(x_+, y_+)$  and  $(x_-, y_-)$  obtained in the Run 1 measurement [1], in this measurement, and for the combination of these two results described in Sect. 8 of the main paper.
- Fig. 2, showing the distribution of the invariant mass of the  $B^+$  ( $B^-$ ) meson in Dalitz bin number  $-4$  ( $+4$ ) for  $B \rightarrow Dh$  candidates in the downstream  $K_s^0$  category, where  $D \rightarrow K_s^0 \pi^+ \pi^-$ . The projections show the result of the fit to extract  $CP$  parameters, described in Sect. 6 of the main paper.  $CP$  violation is visible in the different heights of the  $B^\pm \rightarrow DK^\pm$  signal peaks.

## References

- [1] LHCb collaboration, R. Aaij *et al.*, *Measurement of the CKM angle  $\gamma$  using  $B^\pm \rightarrow DK^\pm$  with  $D \rightarrow K_s^0 \pi^+ \pi^-$ ,  $K_s^0 K^+ K^-$  decays*, JHEP **10** (2014) 097, arXiv:1408.2748.

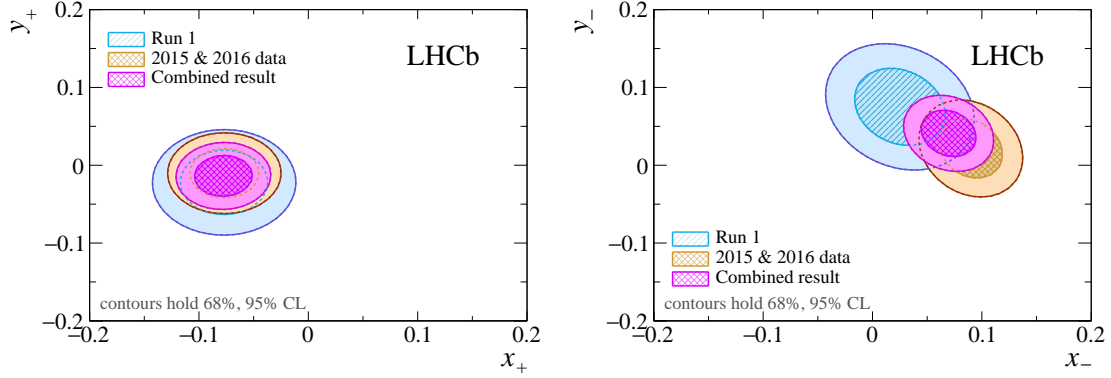


Figure 1: Two-dimensional 68.3% and 95.5% confidence regions for  $(x_+, y_+)$  and  $(x_-, y_-)$  obtained in the Run 1 measurement [1], in this measurement, and for the combination of these two results described in Sect. 8 of the main paper.

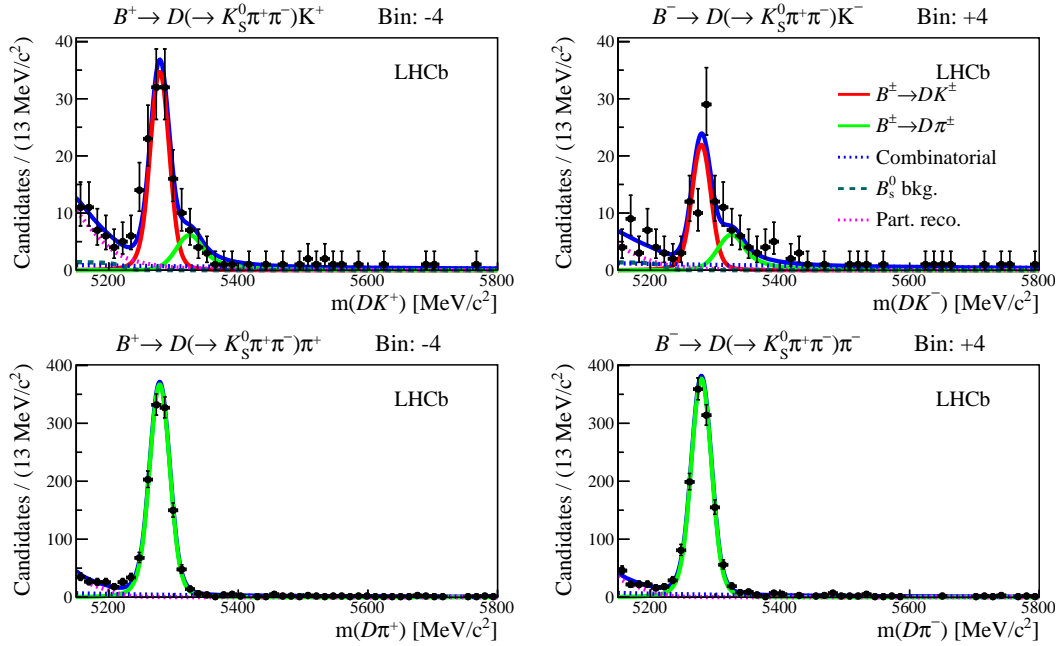


Figure 2: Distribution of the invariant mass of the  $B^+$  ( $B^-$ ) meson in Dalitz bin number  $-4$  ( $+4$ ) for  $B \rightarrow Dh$  candidates in the downstream  $K_S^0$  category, where  $D \rightarrow K_S^0 \pi^+ \pi^-$ . The projections show the result of the fit to extract  $CP$  parameters, described in Sect. 6 of the main paper.  $CP$  violation is visible in the different heights of the  $B^\pm \rightarrow DK^\pm$  signal peaks. The  $B_s^0$  background shape is shown separately in these plots, because it is treated differently from the other partly reconstructed backgrounds in the Dalitz-plot binned fit.